[6]V. S. Suvorov and A. S. Sonin, Zh. Eksperim. i Teor. Fiz. 54, 1044 (1968) [Soviet Phys. JETP 27, 557 (1968)], and references therein.
[7]G. Dolino, J. Lajzerowicz, and M. Vallade, Solid State Commun. 7, 1005 (1969).
[8]R. C. Miller, Phys. Rev. 134, A1313 (1964).
[9]F. Jona and G. Shirane, *Ferrolectric Crystals* (Macmillan, New York, 1962).
[10]Nevertheless, one optical observation has been reported: S. M. Shapiro, R. W. Gammon, and H. Z. Cummins, Appl. Phys. Letters 10, 113 (1967).
[11]Bruhat-Kastler, *Optique* (Masson, Paris, 1965).
[12]L. G. Lomova, A. S. Sonin, and T. A. Regusl'skaya, Kristallografiya 13, 90 (1968) [Soviet Phys. Crist. 13, 68 (1968)].
[13]H. Iwasaki and H. Toyoda, Japan J. Appl. Phys. 7, 787 (1968).
[14]F. Moravets and V. P. Konstantinova, Kristallografiya 13, 284 (1968) [Soviet Phys. Crist. 13, 221 (1968)], and references therein.

PHYSICAL REVIEW B VOLUME 2, NUMBER 6 15 SEPTEMBER 1970

Theory of One- and Two-Phonon Reorientation Rates of Paraelectric Defects in Ionic Crystals*

B. G. Dick and D. Strauch†
Department of Physics, University of Utah, Salt Lake City, Utah 84112
(Received 9 February 1970)

A theory of one- and two-phonon-assisted reorientation rates of substitutional OH^- ions in alkali-halide crystals has been developed. We treat the case of reorientation of dipoles preferring ⟨100⟩ directions with a large static applied electric field in a ⟨100⟩ direction. We use unperturbed breathing shell-model phonons and a dipole-lattice Hamiltonian which includes both one- and two-phonon operators and which is not limited in its validity to the long-wave limit. The theory is applied primarily to OH^- in RbBr with good qualitative agreement with experiment. In particular, we find an approximate T^4 dependence of relaxation rate due to two-phonon Raman-type processes in the 5–10 °K temperature range, in agreement with experiment. Our theory also agrees with experiment in its prediction that two-phonon reorientation processes will begin to dominate one-phonon processes above a temperature of about 4 °K. In the temperature range studied, those two-phonon reorientation rates produced by the one-phonon operators in the dipole-lattice interaction Hamiltonian acting twice exceed by several orders of magnitude the two-phonon reorientation rates produced by the interaction Hamiltonian two-phonon operators acting once. Similar results are found for OH^- in KBr and KCl.

I. INTRODUCTION

There have been several recent studies of the theory of reorientation processes for paraelectric[1,2] and paraelastic[3–6] defects in ionic crystals. These studies all have the feature of using a dipole-lattice interaction Hamiltonian which is valid only for long-wave phonons; also, Debye or other approximate dispersion relations for the phonons have been used. While these approximations are adequate for treating one-phonon-assisted tunneling reorientation processes in attainable electric fields, they are not adequate for two-phonon processes which become important above about 5 °K. In this paper we shall be concerned mainly with an effort to use more realistic models for the phonons and the phonon-defect interaction than have been used heretofore to investigate the one- and two-phonon-assisted tunneling rates of OH^- defects in alkali-halide crystals with a large electric field applied in a ⟨100⟩ direction. We have developed a dipole-lattice interaction Hamiltonian which includes both one- and two-phonon operators and which is not restricted to the long-wave limit, as previously used forms of this interaction Hamiltonian have been. Our treatment gives a very good qualitative account of the temperature and electric field dependence of observed relaxation rates for OH^- in RbBr from 1.35 to 12.5 °K, as well as for OH^- in other alkali-halide hosts for which the relaxation rates are not known over such a wide temperature range. From this study we can acquire new information about the phonon-defect interaction which one hopes may eventually be useful in unraveling some of the puzzles concerning the infrared absorption of these systems.[7] This information also should provide a starting point for a study of the perturbation of the phonons due to

dipolar defects, an effect which is not included in the work described in this paper.

In Sec. II a Hamiltonian for a crystal containing isolated paraelectric defects is described and in Sec. III the dipole-lattice part of this Hamiltonian is discussed. Section IV discusses simplifications arising from the symmetry which the system has when a strong electric field is applied in a ⟨100⟩ direction. Expressions for one- and two-phonon-assisted reorientation rates are developed in Sec. V and methods of numerical calculation are discussed in Sec. VI. Our results are given in Sec. VII, and a summary is provided in Sec. VIII.

II. HAMILTONIAN

OH^- ions enter alkali-halide crystals as substitutional anion impurities. The interesting properties of these systems arise from the permanent electric and elastic dipoles of the defects and the fact that they are easily oriented under applied electric field or stress even at liquid-helium temperatures.

We write the Hamiltonian for a crystal containing a single OH^- substitutional impurity with applied electric and strain fields as

$$H = H_D + H_L + H_{DL} + H_E + H_S \ , \tag{1}$$

where H_D is the Hamiltonian for the OH^- dipole in a static lattice, H_L is that for the phonons, H_{DL} is the dipole-phonon interaction, H_E and H_S are terms describing the interaction of the defects in the crystal with applied electric and strain fields. We now discuss these terms individually in detail. The discussion of H_{DL} is in Secs. III and IV.

There are two complementary ways of treating H_D in use: the Devonshire model[8,9] and the tunneling model.[10–14] Since we are interested only in the lowest motional states of the dipoles, we will use the tunneling model and omit terms describing libration and stretching vibration motion of the dipole. The tunneling model uses a representation in which the six equivalent orientations of the dipole are denoted by $|i\rangle$, where $i = x, \bar{x}, y, \bar{y}, z, \bar{z}$. This is suitable for OH^- in most alkali halides. In this representation, neglecting 180° tunneling, H_D has only off-diagonal matrix elements[10]:

$$\begin{aligned} &\langle i|H_D|j\rangle = 0, \qquad i = j, \quad i = \bar{j} \\ &\langle i|H_D|j\rangle = -\tfrac{1}{2}\Delta, \quad i \perp j, \end{aligned} \tag{2}$$

where Δ is called the tunneling matrix element.

The lattice or phonon Hamiltonian will be taken as that of unperturbed phonons of an ideal host crystal

$$H_L = \sum_\sigma \hbar\omega_\sigma (a_\sigma^\dagger a_\sigma + \tfrac{1}{2}), \tag{3}$$

where σ stands for both wave vector $\vec{q}$ and branch index λ. $a_\sigma^\dagger$ and a_σ are the phonon creation and annihilation operators and ω_σ is the frequency associated with the phonon σ. The eigenstates of H_L are denoted by $\prod_\sigma |n_\sigma\rangle$, where n_σ is the quantum number associated with phonon mode σ. H_L is diagonal in the dipole states $|i\rangle$.

The matrix elements of H_E are[10]

$$\langle i|H_E|j\rangle = -\delta_{ij}\mu_e E_i \ , \tag{4}$$

where E_i are the components of the applied field along the axes associated with the i index. Note that $E_i = E_{\bar{i}}$. μ_e is the external electric dipole moment associated with the OH^- defect in the lattice. The splitting of OH^- tunneling states under action of an applied electric field has been intensively studied.[15,16] What is observed is an energy splitting associated with an applied field. The "external" μ_e deduced from (4) in this way does not give the "microscopic" dipole moment of the defect because of local field effects. So long as one is concerned only with the energy splittings produced by applied E fields, the value of the "microscopic" dipole moment μ is of no concern. However, it will be this μ which will enter into our model for H_{DL}, and we must be prepared to allow μ to differ from μ_e. We note that μ will be composed of the intrinsic OH^- electric dipole moment about its center of charge, a dipole moment due to any displacement of that center of charge from the defect site and any dipole moment associated with lattice distortions produced by the defect. It may also be important to include the effects of zero-point librational motion on μ. The relation between μ and μ_e is discussed further in Sec. VI.

H_S is also diagonal in the directed representation and is given,[2,10] for homogeneous strain, by

$$\langle i|H_S|j\rangle = \delta_{ij}\left(Ae_{ii} + B\sum_{i\neq k} e_{kk}\right) \ . \tag{5}$$

Here e_{ij} are strain tensor components and A and B are coefficients whose difference can be determined from strain dichroism experiments.[17] There is a point connected with the quantity $A - B$ which is similar to that which was just made concerning μ. In the experimental determination of $A - B$, energy splittings for known stresses are measured. Strains appear in (5), so that deduction of $A - B$ from experiment involves use of elastic compliance constants to convert from stress to strain.[2,17] If, owing to lattice relaxation around the defect, the local elastic compliance constants differ from those of the bulk crystal, the $A - B$ deduced from stress experiments will differ from the "microscopic" $A - B$ which we will deduce in Sec. III from the long-wave limit of H_{DL}. This problem is analogous to the local field problem in connection with the electric dipole. Again we must be prepared to consider the possibility that the "microscopic" $A - B$

may differ from the experimental one.

Equation (1) for a single impurity is adequate for treating reorientation rates in crystals containing OH^- defects in sufficiently low concentrations ($< 10^{18}$ OH^-/cc), so that interactions between the defects are known to be negligible.

III. DIPOLE-PHONON INTERACTION

We now derive a form of H_{DL} up to the second order in lattice displacements, i.e., up to two-phonon operators, from a microscopic model of the defect. The model we use is the following: The OH^- is regarded as an object with a dipole moment μ and central Born-Mayer interactions with its nearest neighbors. The H end, the O end, and the sides of the dipoles all have different interactions with the neighbor nearest to them. The corresponding Born-Mayer potential functions are called ϕ_h, ϕ_0, and ϕ_s (see Fig. 1); they are differences between impurity–nearest-neighbor Born-Mayer potential functions and that of the ideal host anion-cation pair. The OH^- center of charge could be taken to be off center, but this does not alter the form of the H_{DL} we will derive, only the interpretation of the coefficients which appear in it. This can be seen in the long-wave limit in Ref. 2.

To deduce an H_{DL} for this model of the OH^- we consider a lattice in which each lattice site occupant, including the OH^-, experiences a displacement $\vec{u}(\vec{L})$, where $\vec{L}$ is the vector specifying the lattice site, the defect site being chosen as the origin. The interaction of the defect with the lattice in this displaced condition comes about due to (i) an electric field at the dipole due to displaced ions; (ii) changes in the nearest-neighbor distances which affect the short-range interactions. The electric field and the Born-Mayer interaction are expanded in powers of the lattice displacements to second order. The interaction of the OH^- with a single ion at site $\vec{L}$ is then given for an OH^- oriented in the [100] direction by

$$[\mu q(\vec{L})/L^3]\{b_x(\vec{L}) - 3l_x[\vec{l}\circ\vec{b}(\vec{L})]\} + \phi_L'[\vec{l}\circ\vec{b}(\vec{L})] \quad \text{(first order)}, \tag{6}$$

$$[\mu q(\vec{L})/L^4]\{\tfrac{15}{2}[\vec{l}\cdot\vec{b}(\vec{L})]^2 l_x - 3[\vec{l}\cdot\vec{b}(\vec{L})]b_x(\vec{L}) - \tfrac{3}{2}b^2(\vec{L})l_x\} + \phi_L'[b^2(\vec{L})/2L] + (1/2L) \times [L\phi_L'' - \phi_L'][\vec{l}\cdot\vec{b}(\vec{L})]^2 \quad \text{(second order)} . \tag{7}$$

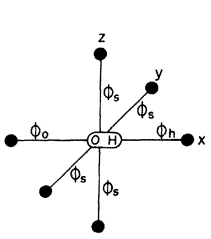

FIG. 1. Born-Mayer potential functions for the short-range interaction of a [100] - oriented OH^- ion with each of its six nearest neighbors.

Here, $q(\vec{L})$ is the charge of the ion associated with lattice site $\vec{L}$, $\vec{b}(\vec{L}) = \vec{u}(\vec{L}) - \vec{u}(0)$ is the displacement of ion $\vec{L}$ relative to the OH^- ion, ϕ_L is the Born-Mayer potential-energy function appropriate for the interaction of the [100]-oriented OH^- with the ion at site $\vec{L}$ ($\phi_L = 0$ except for nearest neighbors), and the primes indicate derivatives of the ϕ's evaluated at the equilibrium separation (the host-crystal lattice spacing) a. $l = \vec{L}/L$.

Summing (6) and (7) over $\vec{L}$ for nearest neighbors we get dipole-lattice Hamiltonian terms $\langle x|H_{DL}^{(1)}|x\rangle$ and $\langle x|H_{DL}^{(2)}|x\rangle$, where $H_{DL}^{(1)}$ is a one-phonon and $H_{DL}^{(2)}$ a two-phonon operator. The neglect of neighbors beyond the nearest is a good approximation when the $\vec{u}(\vec{L})$ are those for long-wave acoustical phonons.[2] We assume this approximation adequate for all phonons. Effects of electronic polarization of lattice ions are omitted from our model for H_{DL}. Off-diagonal matrix elements $\langle i|H_{DL}|j\rangle$ are assumed to be negligible. Evidence for this being a very good assumption will be published elsewhere.[17a] They would correspond to phonon modulation of the tunneling matrix elements. Although $H_{DL}^{(2)}$, in the systems under study here, will turn out to produce a negligible contribution to the two-phonon reorientation rates at the temperatures at which these processes dominate, it is not completely clear at this stage that this is the case and we have carried it through our calculation for the sake of completeness. We have also included a study of $H_{DL}^{(2)}$ since, being quadratic in lattice displacements, it can be regarded as a changed force-constant perturbation of the lattice and may well be of importance in the study of the perturbed phonons of crystals containing OH^- ions.

With the use of the expression for lattice displacements in terms of phonon creation and annihilation operators,[18] we find

$$\vec{u}(\vec{L},\kappa) = \sum_{\vec{q},\lambda}[\hbar/2NM_\kappa\omega_\lambda(\vec{q})]^{1/2}(a_{\vec{q},\lambda}^\dagger e^{-i\vec{q}\circ\vec{L}} + a_{\vec{q},\lambda}e^{i\vec{q}\circ\vec{L}})\vec{w}(\kappa|\vec{q},\lambda) , \tag{8}$$

implying the convention

$$\vec{w}(\kappa|-\vec{q},\lambda) = -\vec{w}^*(\kappa|\vec{q},\lambda)(q\neq 0),$$

$\vec{w}$ being real this way. Then one can write the one- and two-phonon dipole-lattice operators in the forms

$$\langle i|H_{DL}^{(1)}|j\rangle = \delta_{ij}\sum_\sigma[R_i(\sigma)(a_\sigma - a_\sigma^\dagger) + S_i(\sigma)(a_\sigma + a_\sigma^\dagger)] , \tag{9}$$

and similarly for $\langle i|H_{DL}^{(2)}|j\rangle$.

H_{DL} in the form of (8) and (9) is inconvenient for our purposes and will be worked into a more convenient form below. For this reason we will not give the rather lengthy expressions for the coefficients R_i, S_i, etc., in general form. It will be useful, however, to investigate the long-wave part of (9) to show that our $H_{DL}^{(1)}$ in this limit is the same as the long-wave limit used in earlier work on one-phonon relaxation rates and also to establish a connection with H_S. In the long-wave limit[18] ($\vec{q} \to 0$) for the acoustical phonons, $\vec{w}(\kappa|\vec{q},\lambda)/\sqrt{M_\kappa}$ becomes independent of κ, and (8) becomes

$$\vec{u}(\vec{L}) = \sum_{\vec{q},\lambda} [\hbar/2M_c\omega_\lambda(\vec{q})]^{1/2} \times (a^\dagger_{\vec{q},\lambda} e^{-i\vec{q}\cdot\vec{L}} + a_{\vec{q},\lambda} e^{i\vec{q}\cdot\vec{L}})\vec{e}(\vec{q},\lambda) , \tag{10}$$

with M_c being the total mass of the crystal and

$$[\vec{e}(q,\lambda)/\sqrt{M_1 M_2}] = \vec{w}(\kappa|q,\lambda)/\sqrt{M_\kappa} .$$

This form of $\vec{u}(\vec{L})$ is adequate for use in establishing the form of the long-wave part of $H_{DL}^{(1)}$ and has the advantage of somewhat simplifying (9). In this approximation,

$$R_i(\sigma) = R_i(\vec{q},\lambda) = (-1)^{1/2}[\hbar/2M_c\omega_\lambda(\vec{q})]^{1/2} \times [(A/a)e_i(\vec{q},\lambda)\sin q_i a + (B/a)\sum_{j\neq i} e_j(\vec{q},\lambda)\sin q_j a] , \tag{11}$$

$$S_i(\sigma) = S_i(\vec{q},\lambda) = \mathrm{sgn}(i)[\hbar/2M_c\omega_\lambda(\vec{q})]^{1/2} \times [Ce_i(\vec{q},\lambda)(\cos q_i a - 1) + D\sum_{j\neq i} e_i(\vec{q},\lambda)(\cos q_j a - 1)] , \tag{12}$$

where $\mathrm{sgn}(i) = \pm 1$; + for $i = x, y, z$; − for $i = \bar{x}, \bar{y}, \bar{z}$. Here, we have

$$A \equiv (\phi_h' + \phi_0')a , \quad B \equiv 2a\phi_s' , \quad C \equiv 2(\phi_h' - \phi_0') , \quad D \equiv 4\mu e/a^3 . \tag{13}$$

In the long-wave limit $\vec{q} \to 0$, $S_i(\sigma)$ is of order q^2 and Eq. (10) gives, for acoustical phonons,

$$e_{jj} = \frac{\partial u_j}{\partial x_j} = \frac{\partial u_j}{\partial L_j} = \sum_{\vec{q},\lambda_a} i \left(\frac{\hbar}{2M_c\omega_\lambda(\vec{q})}\right)^{1/2} \times q_j e_j(\vec{q},\lambda_a)(a_{\vec{q},\lambda} - a^\dagger_{\vec{q},\lambda}) , \tag{14}$$

so that, using the long-wave limit of (11), we get

$$\langle i|H_{DL}^{(1)}|i\rangle \to Ae_{ii} + B\sum_{j\neq i} e_{jj} . \tag{15}$$

We thus see that H_S is the long-wave acoustical phonon part of $H_{DL}^{(1)}$ and we have a relationship between stress dichroism experiments and the coefficients A and B which occur in $H_{DL}^{(1)}$ subject to the provisos of Sec. I. Equation (13) gives the A and B of (5) in terms of OH^- defect-model parameters. Elasto-optical experiments give

$$A - B = (\phi_h' + \phi_0' - 2\phi_s')a .$$

IV. SYMMETRY CONSIDERATIONS

In the next section we shall be discussing the calculation of reorientation rates of OH^- dipoles occurring under the application of an electric field in a $\langle 100\rangle$ direction. The application of such a field lowers the symmetry of the defect environment from O_h to C_{4v}. In this situation it will be useful to have dipole states and linear combinations of the $\vec{b}(\vec{L})$'s for the nearest neighbors which are basis functions of irreducible representations of the group C_{4v}. This greatly simplifies the calculations of reorientation rates.

In large ($\mu E \gg \Delta$) electric fields parallel to the [100] direction the dipole states can be chosen,[10] neglecting terms of order $\Delta/\mu E$, as

$$\begin{aligned} |1A_1\rangle &= |x\rangle , \\ |2A_1\rangle &= \tfrac{1}{2}(|z\rangle + |\bar{z}\rangle + |y\rangle + |\bar{y}\rangle) , \\ |B_1\rangle &= \tfrac{1}{2}(|z\rangle + |\bar{z}\rangle - |y\rangle - |\bar{y}\rangle) , \\ |1E\rangle &= (1/\sqrt{2})(|z\rangle - |\bar{z}\rangle) , \\ |2E\rangle &= (1/\sqrt{2})(|y\rangle - |\bar{y}\rangle) , \\ |3A_1\rangle &= |\bar{x}\rangle . \end{aligned} \tag{16}$$

These states will be designated by $|m\rangle (m = 1A_1, 2A_1, B_1, 1E, 2E, 3A_1)$ with energies $E_m = -\mu E, 0, 0, 0, 0$, and μE, respectively. They are exact eigenstates of H_E for E parallel to [100].

The appropriate linear combinations of the nearest-neighbor $\vec{b}(\vec{L})$'s will be called symmetry coordinates and are designated by $u_k(\Gamma\gamma)$. Γ stands for one of the irreducible representations of C_{4v}: A_1, A_2, B_1, B_2, or E[19]; γ stands for the row of that representation if it is more than one dimensional, as in the case of E representations which are two dimensional. For the one-dimensional representations, γ can be omitted. k is an index identifying a particular one among several equivalent Γ representations if there are more than one. There are 18 components in all among the six nearest-neighbor $\vec{b}(\vec{L})$'s. The 18-dimensional representation using these components as a basis reduces to four A_1's, an A_2, two B_1's, a B_2, and five E representations. The symmetry coordinates can be written as

$$u_k(\Gamma\gamma) = \sum_{\alpha,\vec{L}} A(\Gamma\gamma k|\vec{L}\alpha)b_\alpha(\vec{L}) , \tag{17}$$

where the sum is over $\alpha = x, y, z$; $\vec{L}$, over nearest neighbors. The coefficients $A(\Gamma\gamma k|\vec{L}\alpha)$ are given

in Table I. The u's, like the b's, are one-phonon operators.

It will be convenient to regard the $u_k(\Gamma\gamma)$ for a given $\Gamma\gamma$ as components of a vector $\vec{u}(\Gamma\gamma)$. These vectors have dimension 4, 1, 2, 1, and 5 for $\Gamma = A_1$, A_2, B_1, B_2, and E, respectively. Equation (17) can then be written as

$$\underline{u}(\Gamma\gamma) = \sum_{\vec{L}} \underline{\vec{A}}(\Gamma\gamma|\vec{L})\vec{b}(\vec{L}) \quad , \tag{18}$$

where the $\underline{\vec{A}}(\Gamma\gamma|\vec{L})$ is nonsquare matrix with components indexed by k and α appearing in Table I.

As will be seen in Sec. V, the dipole states (16) for $m = B_1$, $1E$, and $2E$ play no role in the reorientation processes of interest to us; consequently, we omit consideration of H_{DL} expectation values for these states in the following. $\langle m|H_{DL}^{(1)}|m\rangle$ and $\langle m|H_{DL}^{(2)}|m\rangle$ can be found with the aid of Table I from (6) and (7) summed over nearest-neighbor $\vec{L}$'s. The results for $m = 1A$, $2A_1$, $3A_1$ are in the forms

$$\langle m|H_{DL}^{(1)}|m\rangle = \sum_{\Gamma\gamma} \vec{M}^{(1)T}(m|\Gamma\gamma)\cdot\vec{u}(\Gamma\gamma) \quad , \tag{19}$$

$$\langle m|H_{DL}^{(2)}|m\rangle = \sum_{\Gamma\gamma} \vec{u}^{\,T}(\Gamma\gamma)\cdot \underline{\mathbf{M}}^{(2)}(m|\Gamma\gamma)\cdot\vec{u}(\Gamma\gamma) \quad . \tag{20}$$

Here $\vec{M}^{(1)}(m|\Gamma\gamma)$ is a vector with the same dimension as $\vec{u}(\Gamma\gamma)$ and components $M_k^{(1)}(m|\Gamma\gamma)$ given in Table II. The $\underline{\mathbf{M}}^{(2)}(m|\Gamma\gamma)$ matrices are square matrices with components $M_{kk'}^{(2)}(m|\Gamma\gamma)$ given in Tables III–V. In arriving at (20) we have used the group-theoretic result that there are no cross terms in $\langle m|H_{DL}^{(2)}|m\rangle$ between symmetry coordinates with different $\Gamma\gamma$. In Table II, we find

$$\begin{aligned} p &= \phi_h' - 2\mu e/a^3 \quad , & q &= -\phi_0' - 2\mu e/a^3 \quad , \\ r &= 2\mu e/a^3 , & s &= 2\phi_s' \quad ; \end{aligned} \tag{21}$$

TABLE I. The nonzero coefficients $A(\Gamma\gamma k|L\alpha)$ for expressing symmetry coordinates $u_k(\Gamma\gamma)$ in terms of the components $b_\alpha(L)$, $+x$ being the C_4 axis for the C_{4v} operations.

Γ γ k \ $\vec{L}$ α	(100) x	y	z	(1̄00) x	y	z	(010) x	y	z	(0$\bar{1}$0) x	y	z	(001) x	y	z	(00$\bar{1}$) x	y	z
A_1 1	1																	
2				1														
3							$\frac{1}{2}$			$\frac{1}{2}$			$\frac{1}{2}$			$\frac{1}{2}$		
4								$\frac{1}{2}$			$-\frac{1}{2}$			$\frac{1}{2}$			$-\frac{1}{2}$	
A_2 1								$\frac{1}{2}$			$-\frac{1}{2}$			$-\frac{1}{2}$			$-\frac{1}{2}$	
B_1 1							$\frac{1}{2}$			$\frac{1}{2}$			$-\frac{1}{2}$			$-\frac{1}{2}$		
2								$\frac{1}{2}$			$-\frac{1}{2}$			$-\frac{1}{2}$			$\frac{1}{2}$	
B_2 1								$\frac{1}{2}$			$-\frac{1}{2}$		$\frac{1}{2}$				$-\frac{1}{2}$	
E 1 1	1																	
2				1														
3							$\sqrt{\frac{1}{2}}$			$-\sqrt{\frac{1}{2}}$								
4								$\sqrt{\frac{1}{2}}$			$\sqrt{\frac{1}{2}}$							
5													$\sqrt{\frac{1}{2}}$			$\sqrt{\frac{1}{2}}$		
E 2 1		1																
2					1													
3													$\sqrt{\frac{1}{2}}$			$-\sqrt{\frac{1}{2}}$		
4														$\sqrt{\frac{1}{2}}$				
5								$\sqrt{\frac{1}{2}}$			$\sqrt{\frac{1}{2}}$						$\sqrt{\frac{1}{2}}$	

in Tables III–V,

$$\begin{aligned} a &= 2\beta + \xi_h + \alpha_h \quad , & b &= -2\beta + \xi_0 + \alpha_0 \quad , \\ c &= -\beta + \alpha_h \quad , & d &= \beta + \alpha_0 \quad , \\ e &= -\beta \quad , & f &= \alpha_s \quad , \\ g &= \alpha_s + \xi_s \quad , \\ h &= \tfrac{1}{4}(d + c + 2f) \quad , & i &= \tfrac{1}{4}(a + b + 2g) \quad , \end{aligned} \tag{22}$$

where

$$\begin{aligned} \beta &= 3\mu e/2a^4 \quad , \\ \xi_l &= (a\phi_l'' - \phi_l')/2a \quad , \\ \alpha_l &= \phi_l'/2a \quad , \end{aligned}$$

and no confusion should arise from using a and e as constants on the left-hand sides of (22) as well as for lattice constant and absolute magnitude of the electronic charge on the right-hand sides.

We now proceed to use these expressions for $H_{DL}^{(1)}$ and $H_{DL}^{(2)}$ in a calculation of phonon-assisted tunneling reorientation rates for $1A_1 - 2A_1$ transitions.

V. TRANSITION RATES

We will calculate one- and two-phonon-assisted tunneling transition probabilities among the states $|m\rangle$ for an electric field applied in the $+x$ direction with no applied strain. For the purposes of perturbation theory we group the terms in the Hamiltonian (1) as

$$\begin{aligned} H &= H_0 + H' \quad , \\ H_0 &= H_L + H_E \quad , \end{aligned}$$

with

$$H' = H_D + H_{DL}^{(1)} + H_{DL}^{(2)} \quad . \tag{23}$$

The applied E field is to be considered large in the sense $\mu E \gg \Delta$. The transitions to be considered are transitions between eigenstates for H_0 which we designate $|m\rangle\Pi_\sigma|n_\sigma\rangle$, where the $|m\rangle$ are given by (17).

No transitions occur in first-order perturbation theory since H_{DL} is diagonal in the $|m\rangle$ states and H_D is diagonal in the phonon states. $H_D + H_{DL}^{(1)}$ produces one-phonon-assisted tunneling transitions in second-order perturbation theory. Two-phonon-assisted tunneling transitions occur in second-order perturbation theory because of $H_D + H_{DL}^{(2)}$ and in third-order perturbation theory because of $H_D + H_{DL}^{(1)}$. In calculating transition amplitudes by perturbation theory, one matrix element factor is of the form $\langle m'|H_D|m\rangle$. H_D is the only part of the Hamiltonian (23) which has nonzero matrix elements between different dipole states. From (16)

TABLE II. Nonzero $M^{(1)}(m\,|\,\Gamma\gamma)$ coefficients.

m \ Γ / k	A_1 1	A_1 2	A_1 3	A_1 4
$1A_1$	p	q	r	s
$2A_1$	$\frac{1}{2}s$	$-\frac{1}{2}s$	0	$\frac{1}{2}(s+p-q)$
$3A_1$	$-q$	$-p$	$-r$	s

and (2) it is easy to see that

$$\langle 1A_1|H_D|B_1\rangle=\langle 1A_1|H_D|1E\rangle=\langle 1A_1|H_D|2E\rangle=0$$

and similarly for $3A_1$ replacing $1A_1$ in these matrix elements. The B_1, $1E$, and $2E$ states are thus inaccessible from the $1A_1$ and $3A_1$ states by phonon-assisted tunneling by the H' of Eq. (23). We exclude the B_1, $1E$, and $2E$ states from further consideration and understand, from this point on, that m ranges over $1A_1$, $2A_1$, and $3A_1$ only.

For the reorientation $(m\rightarrow m')$ process assisted by the emission or absorption of a phonon with frequency ω, we find

$$w^{(1)}(m',n_\omega\pm1\,|\,m,n_\omega)=\frac{2\pi}{\hbar}\Delta^2\sum_\sigma\left|\frac{\phi_{m'}(\sigma_\pm)-\phi_m(\sigma_\pm)}{\pm\hbar\omega_\sigma}\right|^2\times\delta(E_{m'}-E_m\pm\hbar\omega_\sigma)\delta(\omega_\sigma-\omega)\,. \quad (24)$$

Here + refers to phonon emission and − refers to phonon absorption,

$$\phi_m(\sigma\pm)\equiv\langle n_\sigma|\langle m|H_{DL}^{(1)}|m\rangle|n_\sigma\pm1\rangle\,, \quad (25)$$

and $n_\omega=(e^{\hbar\omega/kT}-1)^{-1}$. The two-phonon reorientation-process transition rates for specific phonons with frequencies ω and ω' are

$$w^{(2)}(m',n_\omega\pm1,n_{\omega'}\pm1\,|\,m,n_\omega,n_{\omega'})=\frac{2\pi}{\hbar}\Delta^2\frac{1}{2}\sum_{\sigma\sigma'}\left|\frac{\phi_m(\sigma\pm,\sigma\pm)-\phi_{m'}(\sigma\pm,\sigma\pm)}{\hbar(\pm\omega_\sigma\pm\omega_{\sigma'})}+\frac{[\phi_m(\sigma\pm)-\phi_{m'}(\sigma\pm)][\phi_m(\sigma'\pm)-\phi_{m'}(\sigma\pm')]}{\hbar^2(\pm\omega_\sigma)(\pm\omega_\sigma')}\right|^2\times\delta(E_{m'}-E_m\pm\hbar\omega_\sigma\pm\hbar\omega_{\sigma'})\delta(\omega_\sigma-\omega)\delta(\omega_{\sigma'}-\omega')\,, \quad (26)$$

with

$$\phi_m(\sigma\pm,\sigma'\pm)\equiv\langle n_\sigma|\langle n_{\sigma'}|\langle m|H_{DL}^{(2)}|m\rangle|n_\sigma\pm1\rangle|n_{\sigma'}\pm1\rangle\,. \quad (27)$$

In (26) ++ and −− correspond to the emission or absorption of two phonons (summation processes) and +− or −+ correspond to Raman-type phonon processes.

The total transition rates for one- and two-phonon reorientations are given by

$$w^{(1)}(m,m')=\sum_{+,-}\int_0^\infty d\omega\,w^{(1)}(m',n_\omega\pm1\,|\,m,n_\omega)\,, \quad (28)$$

$$w^{(2)}(m,m')=\sum_{+,-}\sum_{+,-}\int_0^\infty d\omega\int_0^\infty d\omega'\,w^{(2)}\times(m',n_\omega\pm1,n_{\omega'}\pm1\,|\,m,n_\omega,n_{\omega'})\,. \quad (29)$$

These can be put into compact forms, useful for computation, in terms of Lifshitz Green's functions.[20] We define the vectors

$$\vec{\chi}(\Gamma\gamma\,|\,\sigma)\equiv\sum_{\vec{L}}\underline{\vec{A}}(\Gamma\gamma\,|\,\vec{L})\frac{1}{\sqrt{N}}\left(\frac{\vec{w}(+\,|\,\sigma)e^{i\vec{q}\cdot\vec{L}}}{\sqrt{M_+}}-\frac{\vec{w}(-\,|\,\sigma)}{\sqrt{M_-}}\right)\,, \quad (30)$$

where + and − refer to anion and cation. In terms of these symmetrized eigenvectors, we can define Green's-function matrices

$$\underline{\mathbf{G}}(\Gamma\gamma,\Gamma'\gamma'\,|\,\omega)\equiv\sum_\sigma\frac{\chi(\Gamma\gamma\,|\,\sigma)\vec{\chi}^\dagger(\Gamma'\gamma'\,|\,\sigma)}{\omega_\sigma^2-(\omega+i\epsilon)^2}=\underline{\mathbf{G}}(\Gamma\gamma\,|\,\omega)\delta_{\Gamma,\Gamma'}\delta_{\gamma,\gamma'}\,, \quad (31)$$

where $\epsilon\rightarrow0+$. Group-theoretic arguments show these to be zero unless $\Gamma'=\Gamma$ and $\gamma=\gamma'$. In the transition rates which we wish to calculate, it is the imaginary part of the Green's functions,

$$\underline{\mathbf{G}}''(\Gamma\gamma\,|\,\omega)=\sum_\sigma\vec{\chi}(\Gamma\gamma\,|\,\sigma)\vec{\chi}^*(\Gamma\gamma\,|\,\sigma)(\pi/2\omega_\sigma)\times[\delta(\omega_\sigma-\omega)-\delta(\omega_\sigma+\omega)]\,, \quad (32)$$

which play a role.

The desired compact forms require two further notational developments: First, we define the vector

$$\vec{\mathfrak{M}}^{(1)}(mm'\,|\,\Gamma\gamma)\equiv\vec{\mathbf{M}}^{(1)}(m\,|\,\Gamma\gamma)-\vec{\mathbf{M}}^{(1)}(m'\,|\,\Gamma\gamma)\,, \quad (33)$$

and also the four-dyadic $\vec{\mathfrak{M}}^{(1)}(mm'|A_1)\vec{\mathfrak{M}}^{(1)T}(mm'|A_1)$. Second, we define a set of matrices $\underline{\mathbf{N}}(mm'|\Gamma\gamma|\omega\omega')$ which have the same dimensionality as $\underline{\mathbf{M}}^{(2)}(\mathrm{m}\,|\,\Gamma\gamma)$ and $\underline{\mathbf{G}}(\Gamma\gamma\,|\,\omega)$, and are given by

$$\underline{\mathbf{N}}(mm'\,|\,\Gamma\gamma\,|\,\omega\omega')\equiv[\underline{\mathbf{M}}^{(2)}(m\,|\,\Gamma\gamma)-\underline{\mathbf{M}}^{(2)}(m'\,|\,\Gamma\gamma)]/\Delta E+[\vec{\mathfrak{M}}^{(1)}(mm'\,|\,\Gamma\gamma)\vec{\mathfrak{M}}^{(1)T}(mm'\,|\,\Gamma\gamma)]/(\hbar^2\omega\omega')\,, \quad (34)$$

where $\Delta E=E_m-E_{m'}$.

Using these definitions we find by straightforward manipulation that (28) and (29) can be written as

$$w^{(1)}(m,m')=\frac{2\Delta^2}{\hbar}\frac{n_{\Delta E}+1}{(\Delta E)^2}\quad\mathrm{Tr}\vec{\mathfrak{M}}^{(1)}(mm'\,|\,A_1)$$

TABLE III. Nonzero $M^{(2)}_{kk'}$ $(1A_1 \mid \Gamma\gamma;\ \Gamma\gamma)$ coefficients.

Γ	γ	k \ Γ′ γ k′	A_1 1	A_1 2	A_1 3	A_1 4	A_2 1	B_1 1	B_1 2	B_2 1	E 1 1	E 1 2	E 1 3	E 1 4	E 1 5	E 2 1	E 2 2	E 2 3	E 2 4	E 2 5
A_1		1	a																	
		2		b																
		3			f	e														
		4			e	g														
A_2		1					f													
B_1		1						f	e											
		2						e	g											
B_2		1								f	c									
E	1	1										d								
		2											f	e						
		3											e	g						
		4													f					
		5														c				
	2	1															d			
		2															f	e		
		3															e	g		
		4																	f	
		5																		f

$$\vec{\mathfrak{M}}^{(1)T}(mm'|A_1)\underline{\mathbf{G}}''(A_1|\Delta E/\hbar)\ , \tag{35}$$

$$w^{(2)}(m,m') = \frac{\hbar\Delta^2}{\pi}\int_{-\infty}^{\infty}d\omega\int_{-\infty}^{\infty}d\omega'\,\delta(-\Delta E+\hbar\omega+\hbar\omega')$$
$$\times(n_\omega+1)(n'_\omega+1)\sum_{\Gamma\gamma}\mathrm{Tr}[\underline{\mathbf{N}}(mm'|\Gamma\gamma|\omega\omega')$$
$$\times\underline{\mathbf{G}}''(\Gamma\gamma|\omega')\underline{\mathbf{N}}(mm'|\Gamma\gamma|\omega\omega')\underline{\mathbf{G}}''(\Gamma\gamma|\omega)]\ . \tag{36}$$

We have used $n_{-\omega}+1=-n_\omega$ in deriving Eqs. (35) and (36), which are valid for both positive and negative ΔE.

The long-wave Debye limit of Eq. (35) can be shown to be

$$w^{(1)}(1A_1, 2A_1) = \frac{\Delta^2(A-B)^2}{20\pi\rho\hbar^4}\left(\frac{2}{c_l^5}+\frac{3}{c_t^5}\right)(n_{\Delta E}+1)\Delta E\ , \tag{37}$$

TABLE IV. Nonzero $M^{(2)}_{kk'}$ $(2A_1 \mid \Gamma\gamma;\ \Gamma'\gamma')$ coefficients.

Γ	γ	k \ Γ′ γ k′	A_1 1	A_1 2	A_1 3	A_1 4	A_2 1	B_1 1	B_1 2	B_2 1	E 1 1	E 1 2	E 1 3	E 1 4	E 1 5	E 2 1	E 2 2	E 2 3	E 2 4	E 2 5
A_2		1	g																	
		2		g			h													
		3			h															
		4				i														
		1					h													
B_1		1						h												
		2							i											
B_2		1								h										
E	1	1									f									
		2										f								
		3											h							
		4												i						
		5													h					
	2	1														f				
		2															f			
		3																h		
		4																	i	
		5																		h

TABLE V. Nonzero $M^{(2)}_{kk'}$ $(3A_1 \mid \Gamma\gamma;\ \Gamma'\gamma')$ coefficients.

Γ	γ	k \ Γ′ γ k′	A_1 1	A_1 2	A_1 3	A_1 4	A_2 1	B_1 1	B_1 2	B_2 1	E 1 1	E 1 2	E 1 3	E 1 4	E 1 5	E 2 1	E 2 2	E 2 3	E 2 4	E 2 5
A_1		1	b																	
		2		a																
		3			f	−e														
		4			−e	g														
A_2		1					f													
B_1		1						f	−e											
		2						−e	g											
B_2		1								f											
E	1	1									d									
		2										c								
		3											f	−e						
		4											−e	g						
		5													f					
	2	1														d				
		2															c			
		3															f	−e		
		4															−e	g		
		5																	g	

where c_l and c_t are longitudinal and transverse sound velocities and ρ is host crystal density. Equation (37) can be compared with Eqs. (8) and (10) of Ref. 2. The rates in Ref. 2 are for $|x\rangle \rightarrow |y\rangle$ transitions and should be multiplied by a factor of 4 to get a $1A_1 \rightarrow 2A_1$ rate. In comparing Eq. (37) above with Ref. 2, we find that a factor $3/16\pi$ has been inadvertently omitted from Eq. (10) there. Correcting this error increases the tunneling matrix elements in column 3, Table I of Ref. 2 by a factor of $(\frac{1}{3}16\pi)^{1/2}$. This reduces the discrepancy between the paraelectric resonance,[21–23] specific-heat,[24] and microwave[25] values of Δ for OH^- in KCl and that Δ deduced from relaxation times, although the latter is still 30% smaller than the former. It should be emphasized that Eq. (37) is an adequate approximation[2] for $w^{(1)}$ for the applied electric fields and temperatures used in the experiments with which we will be comparing our theory.

The long-wave Debye limit of Eq. (36) is

$$w^{(2)}(1A_1, 2A) = \frac{4}{\pi^3}\left(\frac{3\Delta(A-B)^2}{40\rho c_t^5\hbar^2}\right)^2\left(\frac{\kappa T}{\hbar}\right)^3\int_{-\infty}^{\infty}dx$$
$$\times\ x\left(\frac{\Delta E}{\kappa T}-x\right)\frac{e^{\Delta E/\kappa T}}{(e^x-1)(e^{\Delta E/\kappa T}-x-1)}\ . \tag{38}$$

In deriving (38), $H^{(2)}_{DL}$ was set equal to zero, $H^{(1)}_{DL}$ was set equal to its long-wave limit, a Debye phonon spectrum was used, it was assumed that $T \ll \Theta_D$, and the contribution of longitudinal acoustical phonons was omitted. Equation (38) is very similar to but not identical with the two-phonon rates derived by Pirc, Žekš, and Gosar[4] for elastic dipoles. Equation (38) has the required property

$$w^{(2)}(1A_1, 2A_1) = w^{(2)}(2A_1, 1A_1)\epsilon^{-\Delta E/\kappa T}\ ,$$

while the rates of Pirc *et al.* do not.

From Eq. (38) we see that in the long-wave Debye limit and for an experiment in which ΔE is adjusted to equal to κT, $w^{(2)}(1A_1, 2A_1)$ is proportional to T^3. In Sec. VII we show that our calculations, which are not limited to the approximations inherent in (38), yield two-phonon rates proportional to T^n, where n is about 4. Since experiment shows n to be nearer 4 than 3, we see that the long-wave Debye approximation is inadequate for two-phonon processes.

Although we discuss a more detailed calculation in the following sections, it is interesting to attempt to make a rough estimate of the relative importance in $w^{(2)}(m, m')$ of those two-phonon processes produced by $H_{DL}^{(1)}$ acting twice [the second term inside the absolute value in Eq. (26)] compared with those produced by $H_{DL}^{(2)}$ acting once. We will refer to these, respectively, as $w_{1,1}$ and w_2 rates. If these processes were of comparable importance, then the cross term between them $w_{1,2}$, which occurs in the square of the absolute value in (26), would lead to an interesting interference effect in which the rates $w^{(2)}(1A_1, 2A_1)$ and $w^{(2)}(2A_1, 3A_1)$ would be different from one another by just $2w_{1,2}$. Whether such an effect is observable depends on the relative importance of the two kinds of two-phonon processes. From Eq. (6) we see that the contributions to $H_{DL}^{(1)}$ are of the order $\mu es/a$, where $s \sim b/a$ is the strain due to phonons. (On any plausible assumption as to the magnitude of the ϕ', one finds $\phi' \sim \mu e/a^3$.) Similarly, $H_{DL}^{(2)}$ is of the order $\mu es^2/a$. Using these estimates and Eq. (26) we can estimate the ratio

$$w_{1,1}/w_2 \approx (\mu e/a)\Delta E/\hbar^2\omega'\omega \quad , \tag{39}$$

where ω and ω' are the frequencies of the phonons involved in two-phonon process. For Raman processes the dominant phonons participating will be the most abundant, those with $\hbar\omega \sim \kappa T$. Using $\mu \sim 1\ e$ Å, $\Delta E/\kappa \sim 2\ ^\circ$K as typical values for experiments, one finds that the above ratio to be $10^4/T^2 \approx 10^2$ for $T = 10\ ^\circ$K. Thus, for Raman processes, we expect $w_{1,1}$ processes to dominate; the dominance of $w_{1,1}$ should be even stronger for summation processes because of the small frequencies of the phonons associated with them. It appears that the interference effect mentioned above will be unobservable for the systems under study here. The conclusions of this rather rough argument are borne out by more careful calculations, as will be seen in Sec. VII.

VI. NUMERICAL CALCULATIONS

In order to arrive at numerical values for the reorientation rates discussed in Sec. V we need values for the parameters appearing in H_D, H_{DL}, and H_L.

H_D contains only one parameter Δ. It enters into the rates (35) and (36) only as a multiplicative factor Δ^2. One can deduce Δ from the magnitude of relaxation rates in the one-phonon-dominated temperature range if the elasto-optical constant A-B is known. Values of Δ are of relatively minor importance in this paper where our primary concern is with the temperature dependence of relaxation rates rather than with their absolute values.

From (21) and (22) there appears to be a rather large number of unknown parameters in our expressions for H_{DL}. In the combinations in which they appear in (34) there are eight parameters. This number can be reduced if we assume that ϕ_0, ϕ_h, and ϕ_s are all of the Born-Mayer form $\Phi = \lambda e^{-a/\rho}$ with different λ but with $\rho_0 = \rho_h = \rho_s \approx 0.3$ Å. This is probably not a bad assumption judging from the Born-Mayer model for alkali-halide crystals[26] which shows ρ to be about the same for all alkali-ion–halide-ion short-range interactions. If the $\underline{\mathbf{N}}$ matrix (34) is written out explicitly it is found, using this equal-range assumption, that all of the parameters occurring in it can be written in terms of μ, a, $\phi_h' - \phi_s' \equiv \mathfrak{A}$, and $\phi_0' - \phi_s' \equiv \mathfrak{B}$. If one takes μ from electro-optical experiments,[15,16] takes a as the unrelaxed host crystal lattice constant, and takes

$$\phi_h' + \phi_0' - 2\phi_s' = (\mathfrak{A} + \mathfrak{B}) = (A - B)/a$$

from elasto-optical experiments[17] (when available) as discussed in Sec. III, then there remains only a single adjustable parameter in the matrix $\underline{\mathbf{N}}$. Unfortunately, all of these data are not available for the crystals of interest. Available data are given in Table VI. In our calculation we have tried varying μ, $\mathfrak{A}$, and $\mathfrak{B}$ over plausible values beyond the experimental constraints even when data are available. We have discussed in Sec. III the reasons which make this at least permissible.

Since the most extensive experimental data with

TABLE VI. Experimental quantities relevant to H_{DL}.

	μ_e (e Å)	$\mathfrak{A} + \mathfrak{B}$ (10^{-4} dyn)
RbBr	1.0 ± 0.1[a]	(0.7)
RbCl	1.0 ± 0.1	-0.620[b]
KBr	$1.0 + 0.1$[c]	-0.684
KCl	0.92[d]	-0.622

[a]Reference 27.

[b]Values are deduced from the α values of Ref. 17: $\mathfrak{A} + \mathfrak{B} = \alpha/(S_{12} - S_{11})$. The value for RbBr is an estimate.

[c]S. Kapphan and F. Lüty, Solid State Commun. 6, 907 (1968).

[d]I. W. Shepherd, J. Phys. Chem. Solids 28, 2027 (1967).

which our theory can be compared have been taken for OH^- in RbBr with the applied electric field in a $\langle 100 \rangle$ direction, we have focused our attention on this system. Preliminary calculations have also been done for OH^- in KCl and in KBr with results in qualitative agreement with those obtained for OH^- in RbBr. Unfortunately, little is known about perturbation produced by an OH^- defect in RbBr. Estimates can, however, be made. The $\mathfrak{A}+\mathfrak{B}$ value for OH^- in RbBr in Table VI is an estimate based on the known values (based on the assumption of pure crystal $S_{11}-S_{12}$ values) for KCl, KBr, RbCl, and on the observation that $\mathfrak{A}+\mathfrak{B}$ increases slightly on going from KCl to KBr. For low temperatures where one-phonon rates dominate

$$w^{(1)} \propto (\mathfrak{A}+\mathfrak{B})^2 \ ,$$

but at higher temperatures $\mathfrak{A}$ and $\mathfrak{B}$ are needed separately. Their relative importance will be discussed in Sec. VII.

As can be seen from Table VI, μ_e does not vary much from crystal to crystal. As emphasized in Sec. II, however, it is μ and not μ_e which enters our theory. One assumption which one might make would be to suppose that the local field seen by the dipole is the Lorenz local field. If this were the case

$$\mu_e = \tfrac{1}{3}(\epsilon_0+2)\mu \ .$$

This assumption would give $\mu \approx 0.5\,e$ Å ($0.437\,e$ Å for RbBr). Mahan[27] has shown that for substitutional impurities the relationship between μ_e and μ is, in general, more complicated than this.

The phonon information of H_L is contained in the Green's functions (32). We have calculated these using eigenfrequencies and eigenvectors provided by Schröder's breathing-shell model.[28] We replace the δ function in (32) by a rectangular "bin" centered on that one of 100 evenly spaced frequencies

$$\omega_n = (n-\tfrac{1}{2})\omega_{\max}/100 \quad (n=1,\ldots,100)$$

which is closest to $\omega(\vec{q},\lambda)$. Eigenvectors and eigenfrequencies were generated for 1686 different $\vec{q}$ vectors in the Kellerman section,[29] which is $\frac{1}{48}$ of the total Brillouin zone. This corresponds to 64 000 q's in the entire zone. The input data used for the breathing-shell models together with the calculated model parameters are given in Table VII. Core displacements have been used for the ion displacements $\vec{u}$ which appear in the theory. This is consistent with our treatment of H_{DL} in which we have ignored electronic polarization effects.

Because of the low density of states at low frequencies, the error in calculating the Green's-function sums in that region by our method is larger than the error in the standard procedure. This standard procedure of calculating the Green's functions uses equally spaced ω^2 rather than ω, but is inconvenient for calculating the double integral over frequencies in Eq. (36). This situation arises because the ΔE splittings occurring in experiments correspond to rather long-wave phonons. We have instead used a procedure in which we fit the Green's functions at ω_n in the low-frequency region ($\omega_n < 0.06\omega_{\max}$) to the analytical form of the Green's functions appropriate to the long-wave limit. Distributing one-half of the contents of each bin over the two adjacent bins, prior to fitting to the analytic long-wave limit forms, reduces errors produced by accidentally very small or large numbers of frequencies per bin in this range and increases the final results for the rates by only 10 to 20%. This is not a serious computational error in the light of the quantitative discrepancies between our results and experiment. For the same reason, no attempt has been made to further smooth the histogram form for the Green's function which our calculations yield. These histograms were used to calculate the frequency integrals of Eq. (36) by summation over frequency bins.

TABLE VII. Input data and model parameters for the breathing-shell model.[a]

	Unit	RbBr (300 °K)	KBr (0 °K)	KCl (0 °K)
		Input parameters		
m_1	*amu*	85.47	39.102	39.102
m_2	*amu*	79.909	79.916	35.453
r	Å	3.427	3.262	3.116
c_{11}	10^{12} dyn/cm^2	0.315 7	0.418	0.483 2
c_{12}	10^{12} dyn/cm^2	0.049 5	0.056	0.054
c_{44}	10^{12} dyn/cm^2	0.038 4	0.052	0.066 3
α_1	Å^{-3}	1.797	1.201	1.201
α_2	Å^{-3}	4.13	4.13	2.974
Z		0.9	0.9	0.9
ω_T	10^{13} rad/sec	1.70	2.28	2.83
ϵ_0	10^{13} rad/sec	4.87	4.58	4.53
ϵ_∞	10^{13} rad/sec	2.33	2.34	2.16
		Model parameters		
A	$e^2/2a^3$	12.669 0	13.073 80	12.815 77
B	$e/2a^3$	−0.561 10	−0.957 34	−0.896 13
A'	$e/2a^3$	0.033 5	0.704 79	0.551 42
B'	$e/2a^3$	−0.412 22	−0.296 70	−0.244 62
G_1	$e/2a^3$	754.492 25	662.838 66	489.965 53
G_2	$e/2a^3$	321.764 84	184.838 77	191.292 49
Y	$e/2a^3$	−4.135 35	−3.414 76	−3.153 37

[a]See Ref. 25 for details.

VII. RESULTS

In this section we present numerical results of our calculations and compare them with experiment. As will be seen, our theory gives a very good qualitative account of the experimental data but only an approximate quantitative account.

The data of Kapphan and Lüty[30] have been taken for a splitting energy ΔE which is set equal to κT

by adjustment of the electric field which was applied in a ⟨100⟩ direction. They found that this allowed them to set

$$w(1A_1, 2A_1) = \tau^{-1},$$

where τ is the measured quantity with negigible error, thus simplifying the relationship between measured relaxation times and the relaxation rates. For higher fields and/or lower temperatures, the concept of a single relaxation time ceases to be meaningful.[2]

As discussed in Sec. VII, we have varied the parameters μ, $\mathfrak{A}$, and $\mathfrak{B}$ to learn how sensitively calculated rates depend on them. We compare the rates to a "reference" rate based on assuming $\mu = 0.5\,e$ Å, $\mathfrak{A} = \mathfrak{B} = -0.35 \times 10^{-4}$ dyn, and Δ being such as to fit the low-temperature rate to experiment, namely, 7.3×10^{-20} erg. These reference rates are shown[31] in Fig. 2 along with the experimental points of Kapphan and Lüty. Two sets of theoretical curves are shown in Fig. 2. One is for $\Delta E = \kappa T$ for comparison with the experimental data. The other is for a fixed ΔE. From these curves one sees that, as anticipated, Raman two-phonon rates are more important than summation rates, at least by an order of magnitude. From the first set of curves ($\Delta E = \kappa T$) one sees that the one-phonon rate is proportional to T over nearly the whole range between 1 and 10 °K in agreement with the long-wave limit Eq. (37). The summation and Raman two-phonon rates for this case go as T^3 and $T^{4.5}$, respectively, at $T = 10$ °K. The total rate thus is proportional to T at low temperatures going over into a T^4 or $T^{3.5}$ dependence at about 10 °K in approximate agreement with experiment.

Vredevoe[1] has exhibited curves for relaxation rate versus T for OH^- in KCl with a large field in the [111] direction. In the two-phonon region for ΔE held constant he finds a T^{11} dependence. We find an approximate T^4 dependence for constant high field in the [100] direction. There are several reasons for this difference. First, Vredevoe found that for [111] fields $w_{1,1}$ rates vanish in his approximation for H_{DL} so that his rates are of the w_2 type where in our $E\|$ [100] case $w_2 \ll w_{1,1}$. Thus, we have not calculated the same case as Vredevoe has. Also, the model we have used for H_{DL} differs from that of Vredevoe in our inclusion of Born-Mayer repulsions where Vredevoe's model omits them. This leads in Vredevoe's treatment to dipole-lattice interactions proportional, in the long-wave limit, to derivatives of the strain and strain times derivatives of the strain, respectively, for the one- and two-phonon operators which he used to calculate $E\|$ [111] Raman rates. This introduces additional powers of T compared with our model.

Our work confirms Vredevoe's conjecture and our estimates at the end of Sec. V that $w_{1,1} \gg w_2$, that is, that the $H_{DL}^{(1)}$ contributions to two-phonon processes dominate those from $H_{DL}^{(2)}$ for $E\|$ ⟨100⟩. The relative importance of these various contributions, according to our calculations, are shown in Table VIII.

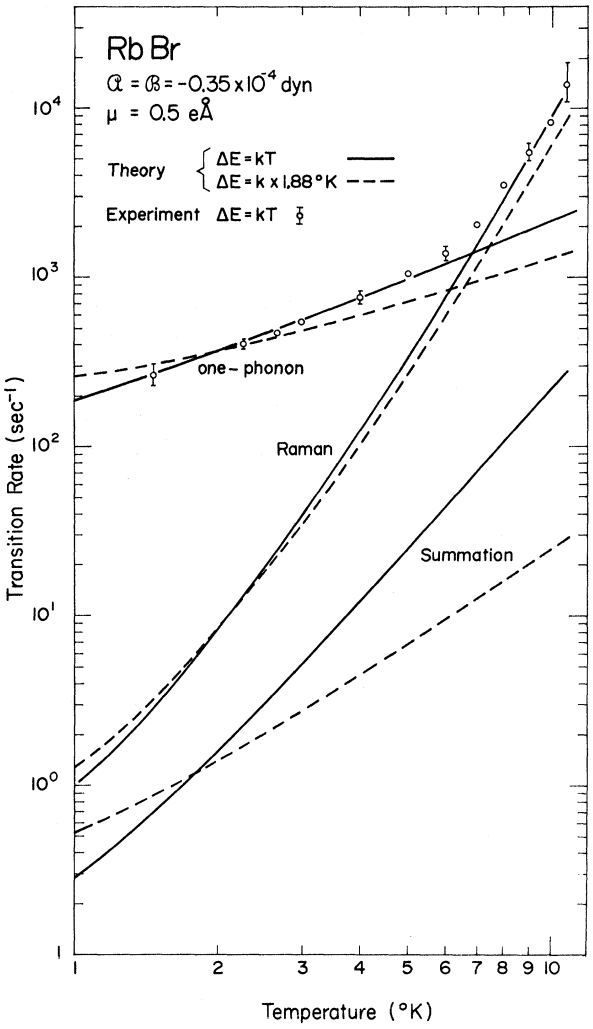

FIG. 2. Reference rates for reorientation of OH^- in RbBr: $\mathfrak{A} = \mathfrak{B} - 0.35 \times 10^{-4}$ dyn, $\mu = 0.5\,e$ Å, $\Delta = 7.3 \times 10^{-20}$ erg. The solid curve is for $\Delta E = \kappa T$. The dashed curve is for $\Delta E/\kappa = 1.88$ °K (applied field 16.1 kV/cm with $\mu_e = 1.0\,e$ Å). The circled points are the experimental points of Kapphan and Lüty for $\Delta E = \kappa T$. One-phonon rates and two-phonon rates of the Raman and summation types are shown separately.

We now discuss the effect on the rates of varying the parameters μ, $\mathfrak{A}$, $\mathfrak{B}$ from the reference values just discussed.

A plot of rates calculated for various values of μ with $\mathfrak{A}$, $\mathfrak{B}$ being held at their reference values is

TABLE VIII. Relative orders of magnitude of various two-phonon processes for $E \| \langle 100 \rangle$.

Process	$\frac{w_{1,1}}{w_2}$	$\frac{w_{1,1}}{w_{1,2}}$	$\frac{w_{1,1}\ \text{Raman}}{w_{1,1}\ \text{Summation}}$
Summation	10^8–10^9	10^4–10^5	10–10^2
Raman	10^3–10^6	10^3–10^4	

shown in Fig. 3. Note that smaller choices for μ give curves in better agreement with experiment. This is evidence supporting the assumption, discussed in Sec. VI, that the Lorentz local field correction needs to be taken into account in relating μ to μ_e. The one-phonon contribution to the rates in the T range where it dominates are insensitive to changes in μ in accordance with results of the long-wave limit calculation Eq. (37) which is independent of μ. The fact that there is a significant μ dependence of rates in the two-phonon range shows that the form of $H_{DL}^{(1)}$ beyond its long-wave limit is playing a role. In the long-wave limit, as we have seen, $H_{DL}^{(1)}$ does not depend on μ.

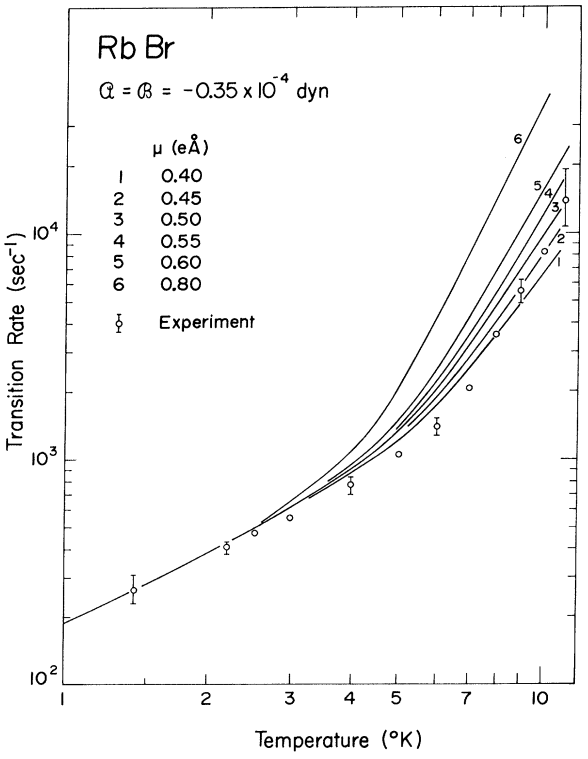

FIG. 3. Total rates for the reorientation of OH^- in RbBr for various values of μ. $\mathfrak{A}$ and $\mathfrak{B}$ have their reference values $\mathfrak{A}=\mathfrak{B}=-0.35\times10^{-4}$ dyn; $\Delta E=\kappa T$.

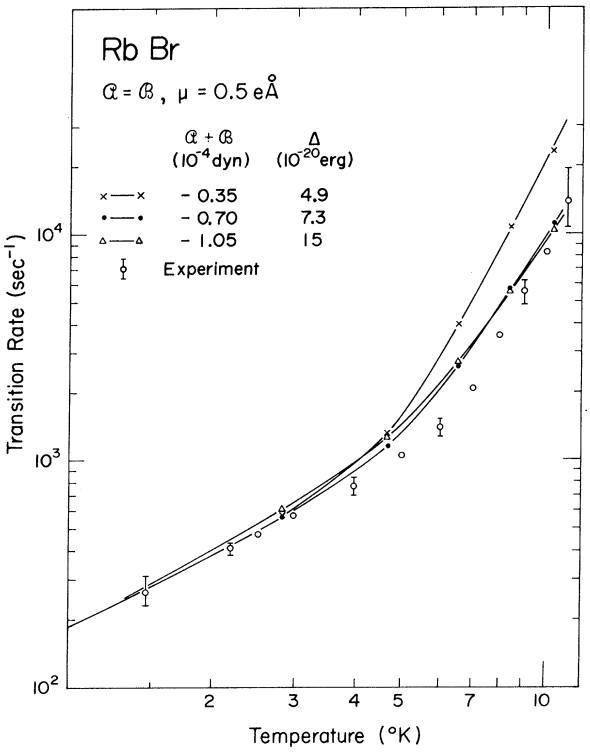

FIG. 4. Total rates for OH^- in RbBr for various values of $\mathfrak{A}+\mathfrak{B}$ ($\mathfrak{A}=\mathfrak{B}$). μ is held at its reference value, 0.5 eÅ; Δ is adjusted for each $A+B$ to fit low-temperature curves to experiment; $\Delta E=\kappa T$.

Figure 4 shows the results of varying $\mathfrak{A}+\mathfrak{B}$ from the reference value while requiring $\mathfrak{A}=\mathfrak{B}$ and holding μ at its reference value. Further, the tunneling matrix element Δ, for each choice of $\mathfrak{A}+\mathfrak{B}$, is adjusted so that low-temperature one-phonon rates which are proportional to $\Delta^2(\mathfrak{A}+\mathfrak{B})^2$ are in agreement with experiment. One sees that decreasing the magnitude of $\mathfrak{A}+\mathfrak{B}$ changes the theoretical curves in a way which gives worse agreement with experiment than the reference case. Increasing $\mathfrak{A}+\mathfrak{B}$ does not much alter the rates, but does reduce the sharpness of the transition from T to T^4 behavior, a transition which is quite abrupt in the experimental curve. Further, the reference case has a slope at higher temperatures which is more nearly that of the experiment than either of the other choices of $\mathfrak{A}+\mathfrak{B}$.

As can be seen from Eq. (35) the one-phonon rates are proportional to the quantity $\mathfrak{A}+\mathfrak{B} = (A-B)/a$. This is of course not the case for two-phonon rates. Our reference choice $\mathfrak{A}=\mathfrak{B}$ ignores the difference between ϕ_0' and ϕ_h' which we expect to exist because of the different electron densities

at the two ends of the OH^- molecule.[32,33] We have varied α and β, holding $\alpha+\beta$ at its reference value, between $\alpha=0$ and $\beta=0$, the results being shown in Fig. 5. Theoretical curves are closer to experimental curves as β approaches zero. This implies $\phi_0' \cong \phi_s'$, which Quigley and Das[29] also found to be a feature of that repulsive interaction which gave them calculated lattice relaxations in better accord with experiment.

VIII. SUMMARY

In this paper we have developed a dipole-phonon interaction Hamiltonian for ⟨100⟩-type paraelectric defects which contains both linear and quadratic terms in lattice displacements and is not limited to the long-wave limit. It is therefore suitable for treating two-phonon Raman and summation processes in phonon-assisted tunneling. We have used time-dependent perturbation theory in second and third order to calculate reorientation rates associated with one- and two-phonon processes in a large ⟨100⟩ electric field.

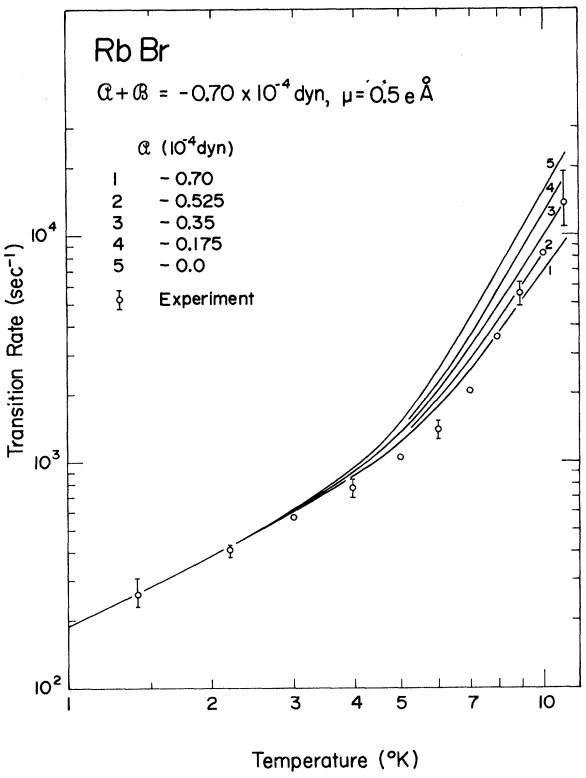

FIG. 5. Total rates for OH^- in RbBr for various values of A and B with $\alpha+\beta=-0.70\times10^{-4}$ dyn. μ and Δ have their reference values; $\Delta E=\kappa T$.

We have found quite good agreement with experiment for OH^- in RbBr. In particular, our theory predicts the observed T and T^4 temperature dependences of rates in those temperature ranges dominated by one- and two-phonon processes and successfully predicts a change from T to T^4 dependence at about 4 °K. We have shown that $w_{1,1}$ two-phonon processes dominate w_2 and $w_{2,1}$ processes in support of a conjecture made earlier by Vredevoe.[1] We have investigated the sensitivity of our results to variation of the three parameters μ, α, and β, which come into our theory. We find that certain values of these parameters give the nearest fit to experiment. These favored values are the following:

(i) $\alpha+\beta$ about the same as the measured values of this quantity for OH^- in RbCl, KBr, and KCl. This is evidence favoring the view that local elastic compliance constants near the defect are not much different from those of pure host crystal.

(ii) $\mu \approx \frac{1}{3}\mu_e(\epsilon_0+2)$. This suggests that the Lorentz local field effect is the dominant effect in determining the relation between the microscopic μ and the external μ_e.

(iii) β is small. This is evidence in support of the view that the sides and the oxygen end of the OH^- molecule repel nearest-neighbor cations with comparable strength and the hydrogen repulsion is stronger than either the sides or the oxygen end.

Our treatment has a number of limitations: Our deduction of H_{DL} is limited to nearest-neighbor interactions and ignores electronic polarization of the lattice and the defect. In view of the rather strong dependence of Raman rates on μ we see that the neglect of electronic polarization may be serious. Probably more severely limiting is our neglect of defect perturbations on phonons in higher order than the second. This neglect can be remedied by use of existing methods of treating such problems and we hope to take up this problem in the future. In this connection we might remark that $H_{DL}^{(1)}$ can be eliminated entirely from the problem by introducing static lattice relaxations.[5,6] $H_{DL}^{(2)}$ and the mass defect represented by the OH^- impurity then produce perturbations in the dynamical matrix of the phonons which previous experience with defects[24–36] has shown might lead to significant effects which are lost in an unperturbed phonon treatment such as ours.

ACKNOWLEDGMENTS

We would like to thank Professor F. Lüty and Dr. S. Kapphan for many useful discussions and for making their experimental data available to us before publication.

*Work supported by the National Science Foundation and by a stipend for one of us (D. S.) from the Deutsche Forschungsgemeinschaft.

†Present address: Physics Dept., Technische Hochschule, München, Germany.

[1]L. A. Vredevoe, Phys. Rev. 153, 312 (1967).

[2]B. G. Dick, Phys. Status Solidi 29, 587 (1968).

[3]J. A. Sussmann, Phys. Condensed Matter 2, 146 (1964).

[4]R. Pirc, B. Žekš, and P. Gosar, J. Phys. Chem. Solids 27, 1219 (1966).

[5]P. Gosar and R. Pirc, in *Proceedings of the Fourteenth Colloque Ampère, Ljubljana* 1966, edited by R. Blinc (North-Holland, Amsterdam, 1967), p. 636.

[6]R. Pirc and P. Gosar, Phys. Condensed Matter 9, 377 (1969).

[7]See, for example, C. K. Chau, M. V. Klein, and B. Wedding, Phys. Rev. Letters 17, 521 (1966); H. Härtel, Bull. Am. Phys. Soc. 13, 499 (1968); M. V. Klein, B. Wedding, and M. A. Levine, Phys. Rev. 180, 902 (1969); G. K. Pandey and V. K. Agrawal, J. Chem. Phys. 50, 1935 (1969); B. Wedding and M. V. Klein, Phys. Rev. 177, 1274 (1969).

[8]A. F. Devonshire, Proc. Roy. Soc. (London) A153, 601 (1936).

[9]P. Sauer, Z. Physik 194, 360 (1966); 194, 478 (1966).

[10]H. B. Shore, Phys. Rev. 151, 570 (1966).

[11]M. E. Baur and W. R. Salzman, Phys. Rev. 151, 710 (1966).

[12]G. Pfister, Helv. Phys. Acta 39, 602 (1966).

[13]P. Sauer, O. Schirmer, and J. Schneider, Phys. Status Solidi 16, 79 (1966).

[14]H. B. Shore, Phys. Rev. Letters 17, 1142 (1966).

[15]U. Kuhn and F. Lüty, Solid State Commun. 2, 281 (1964).

[16]For a review of these and other experiments on the OH^- systems see F. Lüty, J. Phys. Radium C4 Suppl. 28, 120 (1967).

[17]H. Härtel and F. Lüty, Phys. Status Solidi 12, 347 (1965).

[17a]B. G. Dick, Solid State Commun. 8, 777 (1970); see also Ref. 4.

[18]See, for example, A. A. Maradudin, E. W. Montroll, and G. H. Weiss, *Solid State Physics*, edited by F. Seitz and D. Turnbull (Academic, New York, 1963), Suppl. 3, Chap. II. Our wave vectors differ from those in this reference by a factor of 2π.

[19]See M. Tinkham, *Group Theory and Quantum Mechanics* (McGraw-Hill, New York, 1964), p. 325.

[20]See, for example, A. A. Maradudin, I. M. Lifshitz, A. M. Kosevich, W. Cochran, and M. J. P. Musgrave, *Lattice Dynamics* (Benjamin, New York, 1969), p. 53 ff.

[21]W. E. Bron and R. W. Dreyfus, Phys. Rev. Letters 16, 165 (1966); 17, 689 (1966); Phys. Rev. 163, 304 (1967).

[22]G. Feher, I. W. Shepherd, and H. B. Shore, Phys. Rev. Letters 16, 500 (1966); 16, 1187 (E) (1966).

[23]T. L. Estle, Phys. Rev. 176, 1056 (1968).

[24]P. P. Peressini, J. P. Harrison, and R. O. Pohl, Phys. Rev. 182, 939 (1969).

[25]R. S. Scott and W. H. Flygare, Phys. Rev. 182, 445 (1969).

[26]M. Born and K. Huang, *Dynamical Theory of Crystal Lattices* (Oxford U. P., London, 1954), Chap. 1.

[27]G. D. Mahan, Phys. Rev. 153, 983 (1967).

[28]U. Schröder, Solid State Commun. 4, 347 (1966); V. Nüsslein and U. Schröder, Phys. Status Solidi 21, 309 (1967).

[29]E. W. Kellerman, Phil. Trans. Roy. Soc. London A238, 513 (1940).

[30]S. Kapphan and F. Lüty, Solid State Commun. 8, 349 (1970).

[31]The transition rates plotted in the figures are all $\frac{1}{4}w(1A_1, 2A_1) = w(x, y,)$.

[32]R. J. Quigley and T. P. Das (unpublished).

[33]P. Cade, J. Chem. Phys. 47, 2390 (1967).

[34]T. Timusk and M. V. Klein, Phys. Rev. 141, 664 (1966).

[35]J. B. Page, Jr., and B. G. Dick, Phys. Rev. 163, 910 (1967).

[36]D. Strauch and J. B. Page, Jr., in *Localized Excitations in Solids*, edited by R. F. Wallis (Plenum, New York, 1968), p. 567.